

Research paper

Sex differences in the mouse photothrombotic stroke model investigated with X-ray fluorescence microscopy and Fourier transform infrared spectroscopic imaging

J.M. Newton^a, M.J. Pushie^a, N.J. Sylvain^{a,b}, H. Hou^a, S. Weese Maley^b, M.E. Kelly^{a,*}

^a Department of Surgery, College of Medicine, University of Saskatchewan, SK S7N 5E5, Canada

^b Clinical Trial Support Unit, College of Medicine, University of Saskatchewan, SK S7N 0W8, Canada



ARTICLE INFO

Keywords:

Stroke
Sex differences
Cerebral ischemia
Penumbra
Brain metabolism

ABSTRACT

Stroke is a leading cause of death and disability around the world. To date, the majority of pre-clinical research has been performed using male lab animals and results are commonly generalized to both sexes. In clinical stroke cases females have a higher incidence of ischemic stroke and poorer outcomes, compared to males. Best practices for improving translatability of findings for stroke, encourage the use of both sexes in studies. Since estrogen and progesterone have recognized neuroprotective effects, it is important to compare the size, severity and biochemical composition of the brain tissue following stroke in female and male animal models. In this study a photothrombotic focal stroke was induced in male and female mice. Vaginal secretions were collected twice daily to track the stage of estrous. Mice were euthanized at 24 h post-stroke. Histological staining, Fourier transform infrared imaging and X-ray fluorescence imaging were performed to better define the size and metabolic markers in the infarct core and surrounding penumbra. Our results show while the female mice had a significantly lower body mass than males, the cross-sectional area of the brain and the size of infarct and penumbra were not significantly different between the groups. In addition to the general expected sex-linked differences of altered NADH levels between males and females, estrus females had significantly elevated glycogen in the penumbra compared with males and total phosphorus levels were noted to be higher in the penumbra of estrus females. Elevated glycogen reserves in the tissue bordering the infarct core in females may present alternatives for improved functional recovery in females in the early post-stroke phase.

Introduction

Stroke is a leading cause of death and disability around the world, and it is estimated a stroke occurs every three seconds (Feigin et al., 2022). A stroke is the result of reduced oxygen and nutrient supply to an area of the brain. It is classified as either a hemorrhagic stroke, due to a bleeding vessel, or an ischemic stroke, occurring from an occluded artery. While hemorrhagic strokes have a higher mortality rate, ischemic strokes account for approximately 87% of all strokes (Girijala et al., 2017). In ischemic stroke, the central core of the affected area of brain tissue, called the infarct, will die. The surrounding area of tissue, known as the penumbra or peri-infarct zone, is at risk of dying, but is thought to be potentially recoverable. Numerous research teams around the world are working toward better characterization of the penumbra, with the ultimate goal of developing treatments and therapeutic approaches that

could rescue tissue in this region, thereby reducing the stroke burden and potentially improve functional recovery (Yang and Liu, 2021).

The World Stroke Organization outlined the differences in sex in cases of human stroke: females account for 55% of all ischemic stroke and for 52% of all deaths from ischemic stroke (Feigin et al., 2022). Female patients have a higher incidence of stroke and negative outcomes due to stroke, including higher mortality, compared with males (Girijala et al., 2017). Two factors that likely contribute to differences in morbidity and mortality between males and females include a longer average female lifespan compared to males (age is a known risk factor for stroke) and the postmenopausal phenomenon (Haast et al., 2012). During the pre-menopausal age, the stroke incidence between the sexes is comparable, however, there is an increased incidence in female stroke post-menopause (Haast et al., 2012). Also, estrogen has been shown to be protective against cellular death, which is important to consider

* Corresponding author.

E-mail address: m.kelly@usask.ca (M.E. Kelly).

<https://doi.org/10.1016/j.ibneur.2022.07.006>

Received 22 April 2022; Accepted 30 July 2022

Available online 2 August 2022

2667-2421/© 2022 The Authors. Published by Elsevier Ltd on behalf of International Brain Research Organization. This is an open access article under the CC BY-NC-ND license (<http://creativecommons.org/licenses/by-nc-nd/4.0/>).

when conducting research involving energy metabolism (Haast et al., 2012). Other considerations for sex differences in human stroke are variations in physiology. The average female mass is less in most populations, and the clinical presentation of stroke differs in females from males, leading to increased likelihood of delayed diagnosis and treatment (Girijala et al., 2017).

Historically, most of the pre-clinical research has been performed using male animal models and the majority of medical research has been performed on male subjects. In 1993, the US National Institute of Health Revitalization Act was created to ensure women were enrolled in phase III clinical trials and sex differences were considered in these studies (Beery and Zucker, 2011). In 2009, after comparing sex bias favoring male animal research in several biological fields, neuroscience was found to be prominently male-favored (Beery and Zucker, 2011). Historically, female animals have been excluded, in part to reduce experimental complexity resulting in reduced costs with fewer animals. This ostensibly practical approach has the undesirable outcome of generalizing research findings to both sexes, with the underlying assumption, correctly or incorrectly, that findings are likely to be equivalent or insignificant between males and females. This is a contributing factor to the poor translatability of pre-clinical stroke research. (Lyden et al., 2021).

Female rodents have a four day estrous cycle with fluctuating levels of hormones which adds to the complexity of research studies and introduces further experimental variables to consider when studying physiological traits and responses (Wald and Wu, 2010). Tracking the estrous cycle requires daily vaginal smears, which can be a deterrent for researchers considering inclusion of females in their studies if personnel and funding are limited (Wald and Wu, 2010). Before generalizations to both sexes can be made, studies comparing males to females at separate stages of the estrous cycle must be conducted (Beery and Zucker, 2011).

Sex differences in animal studies of blood-brain barrier (BBB) disruption through induced seizures, have shown a higher permeability response in females compared to age-matched males (Oztaş et al., 1992). Further sex-dependent differences on BBB permeability have been reported after nitric oxide (NO) administration, with females displaying a greater response than males. (Diler et al., 2007) Recent studies demonstrated that estrogen binding to receptors on astrocytes of the hippocampus, leads to an elevated level of glycogen with an associated metabolic response which was not observed in male animals (Ibrahim et al., 2020). Neurons derived from young females also demonstrate greater tolerance to the toxic effects of dopamine compared to neurons derived from males and the middle cerebral artery occlusion (MCAO) model generates smaller infarcts in females (Du et al., 2004). The premenopausal phenomenon of ischemic stroke observed in humans has also been demonstrated in rodents resulting in smaller infarct sizes during times of high hormone levels (Manwani and McCullough, 2011). This phenomenon has been heavily studied and reproduced, however, other sex dimorphisms are thought to play a role in ischemic stroke. *In vivo* models of ischemic stroke have shown while females trigger the caspase cascade in response to injury, males activate a caspase-independent cascade resulting in different pathways ultimately leading to cell death (Manwani and McCullough, 2011). Sex differences have also been observed in the peripheral immune response of neurodegeneration after ischemic stroke, as males who underwent splenectomy had a smaller infarct size while female mice did not show the same response (Dotson et al., 2015).

Metabolic markers in post-ischemic brain tissue have been analyzed in male mice using X-ray fluorescence imaging (XFI) and Fourier transform infrared (FTIR) spectroscopic imaging (Caine et al., 2016). XFI is a sensitive technique for measuring the concentration of trace elements *in situ* without the need for sample pre-treatment, while FTIR imaging provides *in situ* detection of a wide range of biomolecules and metabolic markers. Clustering of imaging data from these two techniques allows the infarct, penumbra and the remaining cortex to be differentiated from one another based on the biochemical and

biomarker levels present in these metabolically distinct regions (Pushie et al., 2018a, 2018b; Crawford et al., 2018). Recent studies using these techniques with the photothrombotic (PT) model have shown changes in the post-ischemic tissue over time coincides with an incidence of hemorrhagic transformation of ischemic stroke similar to rates of occurrence in clinical ischemic strokes. (Pushie et al., 2022a) Our previous studies of the elemental and metabolic biomarker composition in the brain after stroke were performed exclusively in male mice. It is therefore important to not only extend new stroke studies to include both sexes in animal models, but to also relate prior work that has been performed exclusively on males to studies that include females (Oztaş et al., 1992). The middle cerebral artery occlusion (MCAO) model of induced ischemic stroke is a strongly favoured model as it mimics a large vessel occlusion stroke, however the model has been shown to generate larger stroke lesions in male mice compared with females (Cordeau et al., 2008). We therefore chose to employ the PT stroke model in the current study for the highly reproducible stroke lesion location and volume that it generates in order to minimize variation in stroke severity between subjects. Focusing on elemental and biomarker changes at 24-hours post-stroke we identified glycogen and phosphorus were significantly different between females and males, with females demonstrating elevated glycogen in the ischemic penumbra.

Methods

Animal care and estrous cycle tracking

11-week-old BALB/c male ($n = 18$) and female ($n = 22$) mice had access to chow and water and were housed in a 12 h light/dark cycle (Winship and Murphy, 2008). The University of Saskatchewan Animal Research Ethics Board approved the project and the Canadian Council on Animal Care guidelines were followed. Vaginal smears were performed twice daily to identify the stage of estrous cycle. The samples were collected by flushing the vagina using 10 μ L of normal saline, and then letting the saline dry onto glass slides. Slides were stained with hematoxylin and eosin (H&E) and then viewed under the microscope to determine the stage of the reproductive cycle based on previously described methods (Caligioni, 2009). Surgeries were planned in either the diestrus or estrus phase.

Photothrombotic stroke model

Isoflurane was used for an anesthetic during the procedure (2% induction, 1.5–2% maintenance in 40/60 O₂/N₂O, Baxter Corporation, CA). The top of the skull was shaved with a handheld razor (Braun Cruzer, Procter & Gamble, CA) and a stereotaxic frame secured the head. A RightTemp® temperature monitor and homeothermic controller (Kent Scientific Corporation, USA), were used to monitor body temperature throughout the procedure. Vital signs such as respiratory rate, heart rate and oxygen saturation were monitored using a MouseOX Plus (Starr Life Sciences Corp., USA). The skull was exposed following a midline incision in the scalp. Bregma was used to identify the primary somatosensory cortex (S1FL, at coordinates -1 to -2.5 mm midline to lateral; $+1$ to -0.5 anterior to posterior of the bregma, right hemisphere). Rose Bengal (100 mg/kg bodyweight, Sigma, USA) was injected intraperitoneally, followed by a 5 min wait to let it enter systemic circulation. To reduce scattering of the laser light, a sterile mask was placed on the surrounding area of the primary somatosensory cortex. To photoactivate the Rose Bengal, a green laser (532 nm) illuminated the S1FL for 20 min (average power density was 23 mW), with the laser source positioned 3 cm above the skull. Post-stroke time zero is recorded as the time the laser is powered off. Prior to suturing, marcaine (2 mg/kg, administered at 1.67 mg/mL in saline) was applied to the open incision and saline was administered subcutaneously (0.01 mL/g) immediately after suturing. Animals were monitored in single animal cages during recovery and given additional saline (0.25 mL) subcutaneously 4 h after surgery. In

sham animals, the same procedures were followed but the laser was not powered on. A total of 6 estrus and 6 diestrus PT stroke females were generated and 13 PT stroke models generated in the male group, with an additional 5 male shams and 10 diestrus female shams.

Inclusion criteria for the stroke treatment group was any sign of ipsilateral forelimb weakness post-stroke, while exclusion criteria for this group was any lack of forelimb weakness, indications of contralateral forelimb weakness, the inability to walk, or circling while walking. Inclusion criteria for the sham treatment group was equal forelimb strength, while exclusion criteria for this group was any limb weakness, inability to walk, or circling while walking. During the 24-hour post-stroke period the animals were left to recover and were not subjected to further testing beyond those required for inclusion/exclusion in the study.

Tissue preparation

Animals were euthanized at 24-hours post-stroke by decapitation following heavy sedation with isoflurane. The heads were immediately submerged in liquid nitrogen to preserve biochemical speciation and distribution of labile ions in the brain (Hackett et al., 2011). The animal tissue and skull were chiseled away from the frozen brain while heads were maintained at *ca.* -20°C . The brains remained frozen in the cryomicrotome and were mounted for sectioning. The brains were not immersed in buffers or subjected to other rinsing steps, which follows the preferred tissue preparation methods for elemental mapping (Pushie et al., 2022b). Starting $+0.25$ mm anterior to bregma, coronal brain sections were obtained using a cryomicrotome, at an operating temperature of -18°C .

Disposable polytetrafluoroethylene (PTFE) coated Tissue-Tek Accu-Edge microtome blades (Sakura Finetek USA, Inc., USA) were used for sectioning. The tissues from experimental groups were assigned a randomized numerical identifier during this process. For histology, the tissue sections were collected on glass microscope slides at $14\ \mu\text{m}$ thick. Sections for FTIR imaging were collected onto CaF_2 discs at $10\ \mu\text{m}$ thick. Opaque plastic microscope slide storage boxes were used for storage of all FTIR sections in the dark at -80°C until imaging. Adjacent coronal sections for XFI were collected on trace element-free Nunc Thermanox coverslips (Thermo Fisher Scientific Inc., USA) at $30\ \mu\text{m}$ -thick, and the tissue was allowed to air-dry at ambient temperature before analysis. Buffers, washes or tissue fixation was not used on any sections for XFI or FTIR as these steps are known to alter the underlying distribution and concentration of metabolites *in situ* (Hackett et al., 2011; Pushie et al., 2022b).

Histology & microscopy

Coronal brain sections on glass slides were fixed in 4% buffered paraformaldehyde, washed with 0.1 M phosphate buffered saline (PBS), and then stained with H&E as previously described (Caine et al., 2016; Pushie et al., 2020). Leica Aperio virtual microscope was used to image the H&E-stained tissues with a 20x objective lens and images were extracted using Aperio ImageScope (Leica Biosystems Inc., CA).

Fourier transform infrared spectroscopic imaging & data processing

FTIR spectroscopic imaging was carried out at the Mid-IR beamline at the Canadian Light Source (CLS) synchrotron in “off-line” mode with a thermal globar source using a Hyperion 3000 microscope fitted with an upper objective of $15\times$ magnification and a numerical aperture of 0.4, and a lower condenser of $15\times$ magnification and 0.4 numerical aperture – affording a pixel size of $2.65\times 2.65\ \mu\text{m}$. Data was subjected to 8×8 pixel binning, yielding an effective pixel size of $21.2\times 21.2\ \mu\text{m}$ in the final images. Data was acquired as the average of 16 accumulated scans over the $3900-900\ \text{cm}^{-1}$ range with $4\ \text{cm}^{-1}$ spectral resolution. A background image (blank) was collected from a region of empty CaF_2

substrate using an average of (Gaignard et al., 2018) scans immediately prior to each sample.

Data was processed using the Python-based data mining and visualization application Quasar (Demsar et al., 2013). Integrated peak intensities provided quantitative measurements of lipids ($1715-1755\ \text{cm}^{-1}$), total protein ($1610-1690\ \text{cm}^{-1}$), glutamate (and aspartate: $1565-1590\ \text{cm}^{-1}$), and infrared attenuation ($1800-2250\ \text{cm}^{-1}$). Second derivative spectra were generated with 13 point smoothing and a second order polynomial for aggregated protein (represented as β -sheet secondary structure: $1625\ \text{cm}^{-1}$), lactate ($1127\ \text{cm}^{-1}$), NADH ($1666\ \text{cm}^{-1}$), $\beta\text{-PO}_2$ (indicative of ATP and ADP: $1240\ \text{cm}^{-1}$), and glycogen ($1152\ \text{cm}^{-1}$) following vector normalization to the protein region ($1590-1710\ \text{cm}^{-1}$). Multi-dimensional clustering, performed in Quasar, (Demsar et al., 2013) utilized lipid, protein, aggregated protein, glycogen and lactate content to obtain region(s) of interest (ROIs). Due to the high signal-to-noise between on-sample and off-sample areas for some metabolites, the relative pixel intensity off-sample area from the protein map was used to mask all FTIR maps for visualization. All analysis was performed on non-masked data.

X-ray fluorescence imaging & data processing

XFI was carried out at the Stanford Synchrotron Radiation Light-source (SSRL) on beamline 10-2, with the SPEAR3 storage ring operating in top-up mode at 3 GeV and 500 mA. Beamline 10-2 was equipped with a 33-pole 1.45-T wiggler, using a Si(111) double-crystal monochromator ($\phi = 90^{\circ}$ orientation) and a Rh-coated mirror for focusing. A microfocussed beam was achieved using an aperture downstream of the I_0 ion chamber, followed by a microfocussing polycapillary, with a spot size at the sample of *ca.* $35\ \mu\text{m}\times 35\ \mu\text{m}$. Samples were mounted at 45° to the incident beam and raster scanned using Newport IMS Series stages (Newport Corp., USA) in $30\ \mu\text{m}$ steps, providing an oversampling pixel size of $30\ \mu\text{m}$, at a data acquisition time of 200 ms per point. Imaging used an incident energy, 13,450 eV, below the Br K-edge. A silicon drift Vortex detector was positioned 45° to the sample normal (90° to the incident beam). The detector was fitted with a collimator to reduce total counts from scattered X-rays in the sample area and the Xpress3 signal processing system (Quantum Detectors, UK) was used to obtain the full multi-channel array spectrum for each pixel for off-line processing.

Multi-channel array spectra at each data point in the XFI maps were processed using the MicroAnalysis Toolkit (SMAK), which fits the total X-ray fluorescence emission spectrum using a series of emission lines for each element (Webb, 2011). The fitted X-ray fluorescence intensities were converted to aerial concentrations ($\mu\text{g}/\text{cm}^2$) in SMAK using reference standards deposited on $6.3\ \mu\text{m}$ -thick mylar film. Standards include: K and Cl (KCl, $98.8\ \mu\text{g}/\text{cm}^2$), Ca (CaF_2 , $56.8\ \mu\text{g}/\text{cm}^2$), P (GaP, $47.0\ \mu\text{g}/\text{cm}^2$), Fe (Fe, $56.0\ \mu\text{g}/\text{cm}^2$), S and Cu (CuS_x , $\text{Cu} = 74.9\ \mu\text{g}/\text{cm}^2$, $\text{S} = 21.0\ \mu\text{g}/\text{cm}^2$), and Zn (ZnTe , $45.8\ \mu\text{g}/\text{cm}^2$) (Micromatter Technologies Inc., CA). Multi-dimensional clustering to obtain ROIs utilized P, S, Cl, K, Fe, and Zn data and was performed in Quasar (Demsar et al., 2013). The relative pixel intensity from the off-sample area from the K map was used to mask all XFI maps for visualization, although analysis was performed on non-masked data.

Statistical analysis

Physiological parameters as well as elemental concentrations and FTIR biomarkers were compared between ROIs and the data was found to be nonparametric in distribution using the Shapiro-Wilk test. Significant differences, corresponding to a 99% confidence interval (p value ≤ 0.01) were identified using the Kruskal–Wallis nonparametric analysis of variance method, followed by a *post-hoc* test of multiple comparisons using the Conover-Iman method as implemented in the software package StatsDirect (StatsDirect Ltd., UK) (Kruskal and Wallis, 1952; Conover and Iman, 1979; Conover, 1999) All p -values are reported in

Tables S1, S2, and S3 in Supporting Information.

Results

Histological findings

H&E staining of coronal tissue sections (schematic reference shown in Fig. 1A) at 24-hours post PT stroke from males, estrus and diestrus females (Fig. 1B, C, and D, respectively) reveals poor staining in the right somatosensory cortex, with a clear distinction from the surrounding tissue. Ischemia induces pan-necrosis and selective neuronal necrosis in the affected tissue, with the most significant changes confined to the infarct core. While there is an identifiable demarcation between the infarct core and the surrounding tissue in the H&E images, the precise extent of any peri-infarct zone or penumbra is not evident and cannot be visualized with this technique.

Gaussian-based clustering of metabolic images

Elemental concentrations and their distributions were used to inform

Gaussian-based cluster analysis of XFI data to identify ROIs in elemental maps. Clustering differentiated the infarct core (infarct) from a surrounding region (penumbra) in all PT cases (Fig. 1B, C, and D). XFI clustering employed P, S, Cl, K, Ca, and Zn data to identify ROIs. Similar clustering of FTIR spectroscopic imaging maps (not shown) also identified the infarct core, albeit with a narrower penumbra border surrounding the infarct. The infarct and penumbra were compared against an isolated sub-region of the remaining ROI (which encompassed all unaffected tissue) taken from the cortex contralateral to the PT stroke lesion.

General trends in metabolic markers from XFI and FTIR imaging

Comparing quantified biomarkers between estrus and diestrus females and males, in either the stroke treatment group (PT) or animals in the sham group, demonstrated few significant differences (see Table S1 in Supporting Information). In nearly all instances, the biomarker levels in the contralateral cortex of the male and female PT stroke animals (regardless of the female estrous cycle stage) show no significant differences with any of these animal groups in the sham population.

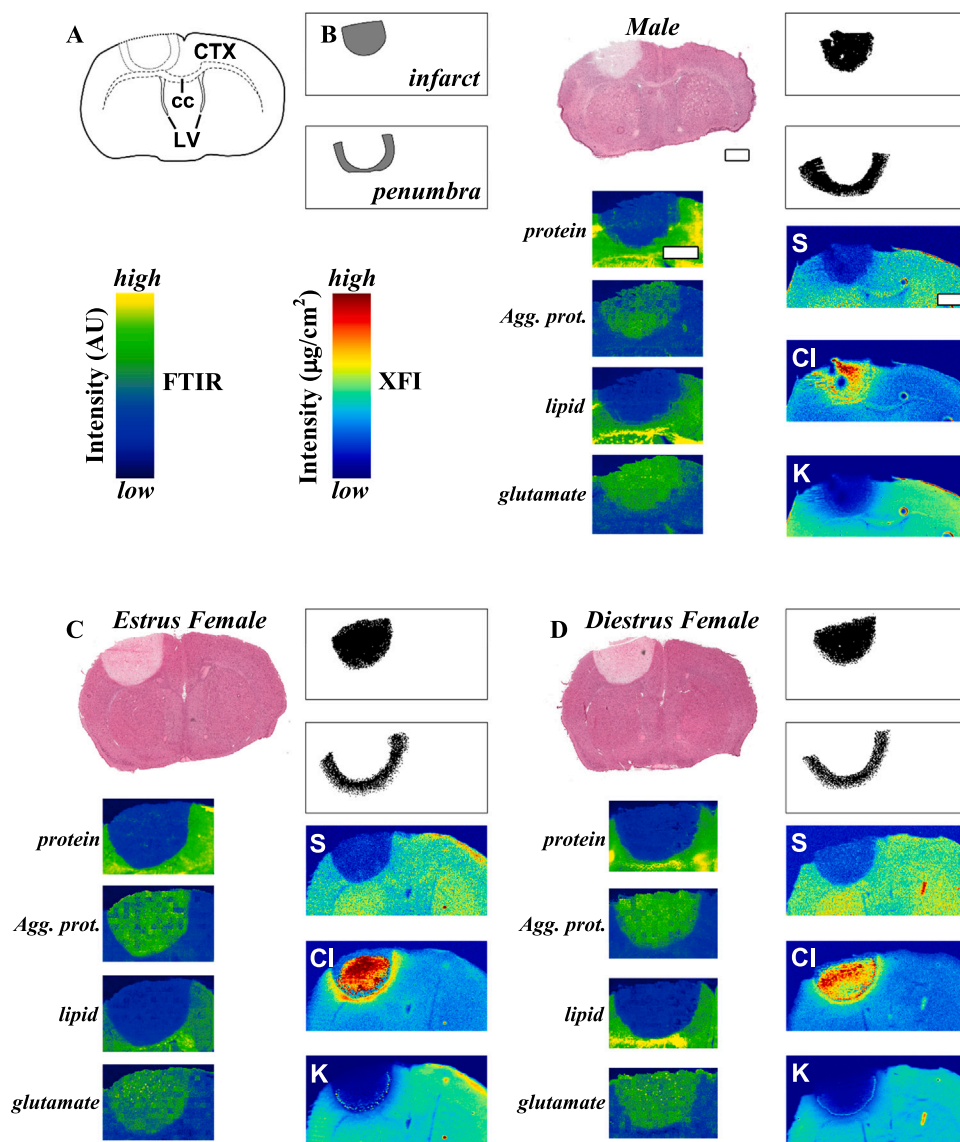


Fig. 1. Schematic depiction of coronal brain sections, ROIs, and colour scales (A). Comparison of male (B) and estrus (C) and diestrus (D) female PT stroke brain sections at 24-hours post-stroke. Representative metabolites and elemental maps from FTIR spectroscopic imaging and XFI, respectively. Scale bars in B for H&E, XFI, and FTIR images denote 1 mm.

Notable exceptions were NADH from FTIR imaging and Cu from XFI. NADH demonstrated differences between males and females (regardless of estrous state), but this difference is isolated to the PT group, as the shams only showed a trend toward this same pattern, but did not reach statistical significance (Table S1E). The Cu levels demonstrated some significant differences between male and estrus female PT and sham groups, as well as trends toward significant differences between estrus and diestrus females (PT and sham) and between the diestrus females and the male sham group. Further analysis of the off-sample Cu levels (background) demonstrated identical trends in significance between the identified groups, indicating Cu levels in these experiments were not reliable (cortex levels of Cu are close to the detection limits of the XFI methods employed and therefore subject to greater error).

Many of the markers analyzed with XFI and FTIR do not show any significant level differences between male and female groups, including when the female estrous cycle is taken into account, for comparisons between infarct, penumbra, or contralateral cortex. Nevertheless, within

each group (males, estrus, or diestrus females) the metabolite levels in the cortex are nearly always significantly different from levels in the penumbra, and the infarct demonstrates significant differences from metabolite levels in the penumbra (summarized in Table S3 in Supporting Information).

The concentrations of nine different metabolites were analyzed with the FTIR data collected. These metabolites included lipids, lactate, aggregated protein, protein, NADH, glycogen, glutamate, ATP+ADP, and IR attenuation. Fig. 1 shows representative distribution images of protein, aggregated protein, lipids, and glutamate. The elements collected for XFI data analysis include phosphorus, sulfur, chlorine, potassium, calcium, iron, copper and zinc. In Fig. 1, the total sulfur, chlorine and zinc maps are shown as representative examples. The FTIR and XFI images in Fig. 1 represent of the type of contrast these methods provide for visualizing infarcted tissue.

All of the metabolites listed above for both FTIR and XFI were used to compare concentrations of the contralateral cortex between all PT stroke

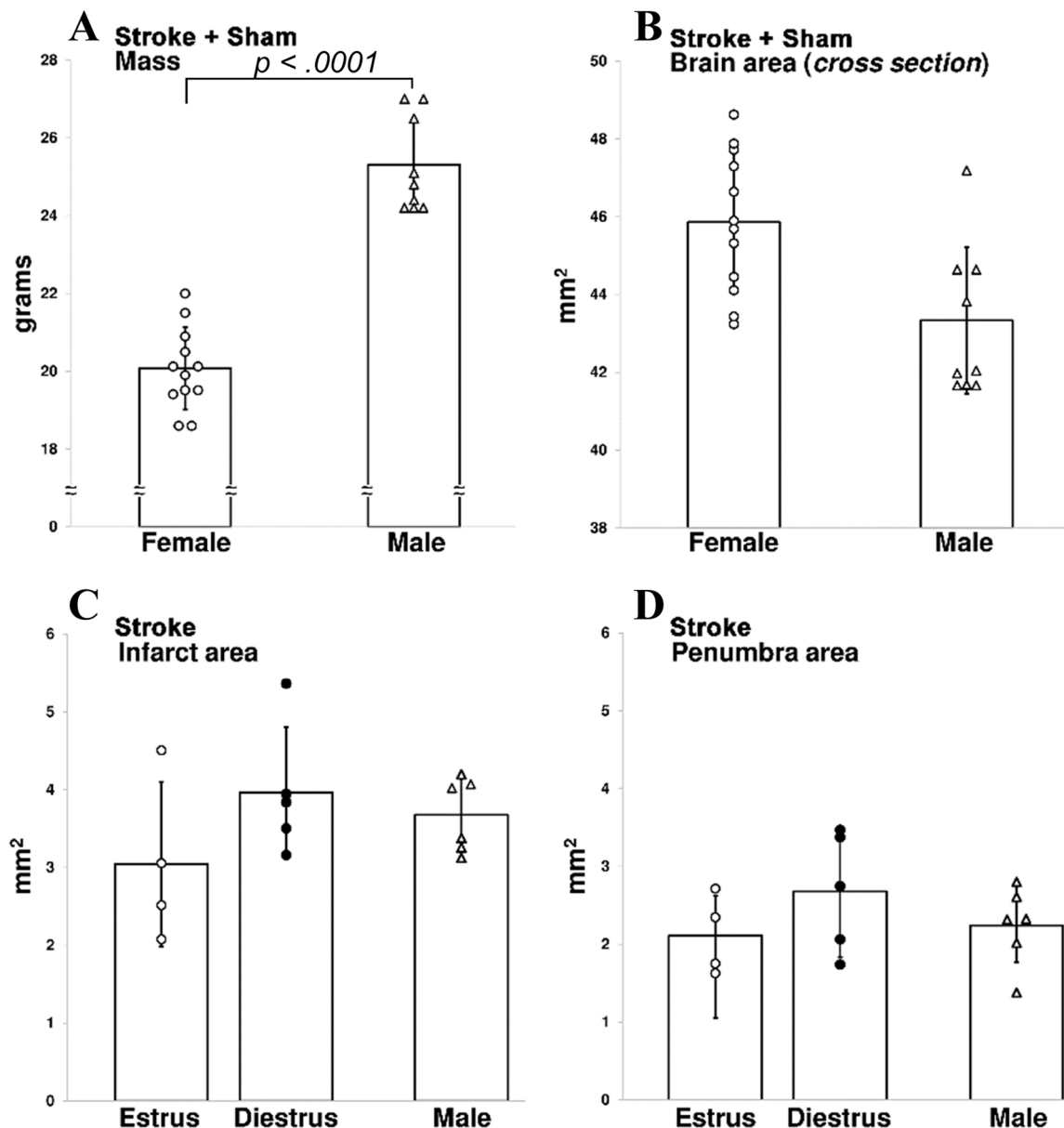


Fig. 2. Comparison of female and male physiological parameters. Mass values were recorded pre-stroke, while the cross-sectional areas of the brain sections are recorded after euthanization (24-hours post surgery) and includes both PT stroke models and shams. The cross-sectional area of the infarct and penumbra are recorded from tissue used to collect XFI data and after clustering analysis and do not include shams. Only mass showed a significant difference between males and females ($p = <0.0001$).

groups and sham animals. As shown in Table S1, there was no significant difference between groups (p -values > 0.01) aside from NADH. Estrus and diestrus PT animals had significantly higher NADH than male PT animals in the contralateral cortex. Differences were also observed between estrus sham and male PT animals, as well as between male sham and diestrus sham. For the remainder of analysis, the male and female cortex reference values used the contralateral cortex values from both sham and PT animals for each sex due to their lack of statistically significant differences (see Table S1).

Physiological parameters

11-week-old male and female BALB/c mice were weighed prior to PT or sham surgeries, with females weighing an average of 16.5% less than males ($p < 0.0001$, Fig. 2 A, p -values summarized in Table S2A in Supporting Information). Once the brains were removed post-mortem the midbrain cross-sectional area at the approximate centre of the PT lesion in all animals, was assessed with digital microscopic imaging (pixel resolution = 10 μ m). No significant difference in the cross-sectional area of the coronal brain sections were found between estrus and diestrus females, while the male and female groups demonstrated a 2.2% difference in cross-sectional area (Fig. 2 B), which was not significant (Table S2B). This demonstrated there was no significant difference in brain size observed between male and females.

Infarct core and penumbra size

The cross-sectional area of the infarct core (as identified from cluster analysis from the subset of specimens subjected to XFI) revealed no significant differences between estrus or diestrus phases of the reproductive cycle in females, nor between these groups and the male group (Fig. 2 C, p -values in Table S2C), nor were any significant differences observed between these groups when analyzing the cross-sectional area of the penumbra (as identified from XFI clustering, Fig. 2 D, p -values in Table S2D). While there appears to be a trend toward slightly larger infarct and penumbra areas in the diestrus female group (Fig. 2 C and D), the total area of affected tissue (sum of infarct+penumbra) was not significant across any of the 3 groups (p -values in Table S2E).

Significant differences among female and male PT stroke models

Fig. 3A demonstrates a representative example of significant differences in lipid levels between infarct and penumbra, between infarct and cortex, and between penumbra and cortex within all 3 groups (estrus or diestrus females and males, Fig. 3A, p -values listed in Table S3A). The lipids markers also present a useful example of insignificant differences when comparing the infarct ROIs between each of these three groups. Moreover, these 3 groups demonstrated insignificant differences in lipid levels when comparing each of the penumbra ROIs, or when comparing the levels of lipids between the cortex of males and females (Fig. 3A).

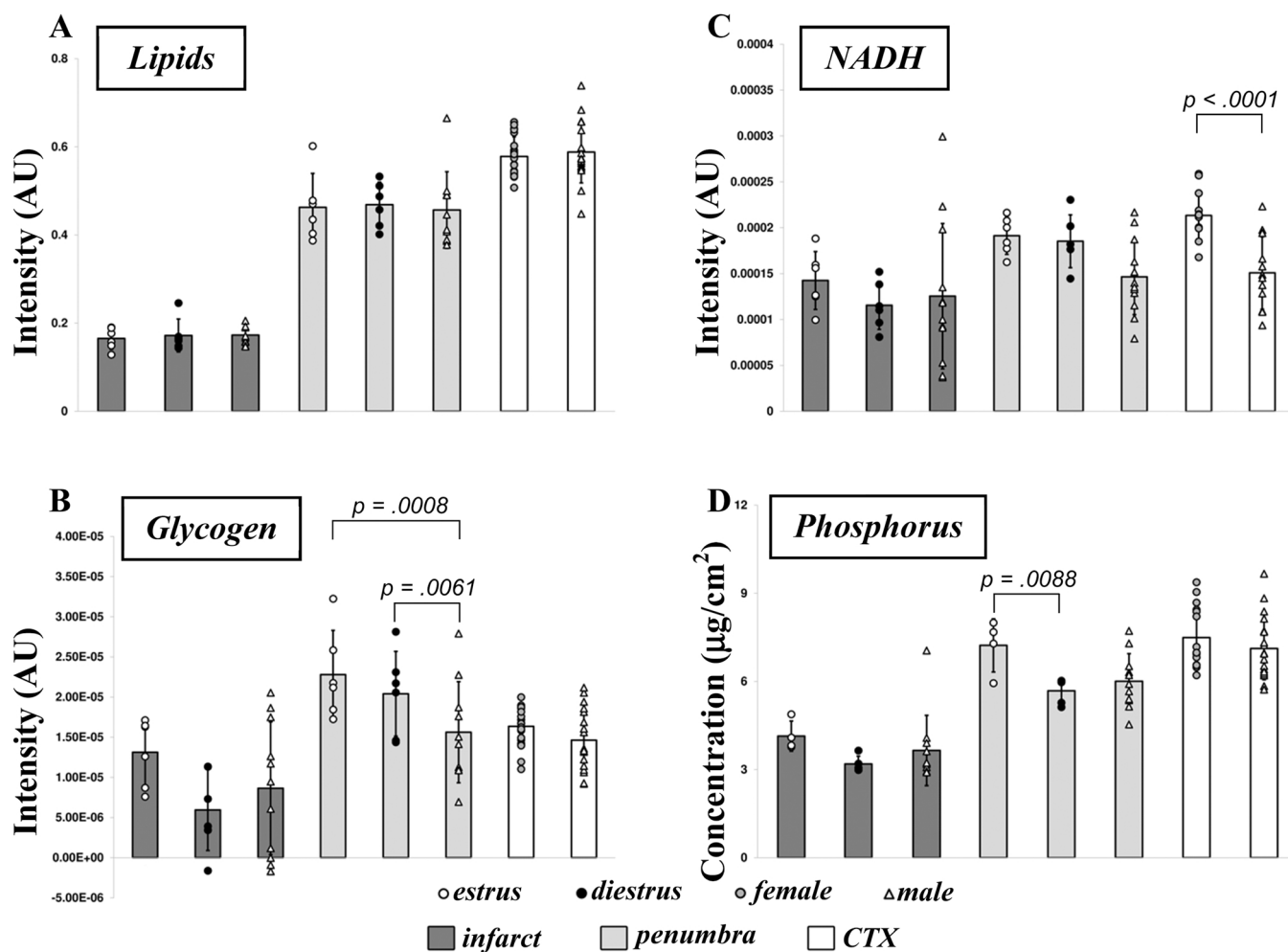


Fig. 3. Comparison of post-stroke metabolite levels between infarct, penumbra, and cortex (CTX) in females (estrus and diestrus) and males. Cortex values represent the contralateral cortex of PT stroke specimens as well as shams. Contralateral cortex and sham cortex levels (Table S1) were shown to be comparable in all cases except for Cu (due to detection limit issues) and NADH (due to known sex differences in mitochondrial respiration).

The majority of biomarkers analyzed, with the exception of NADH (Table S3E), glycogen (Table S3F) and phosphorus (P, Table S3J), did not show significant differences between male and female infarcts, nor were there differences for the remaining markers when comparing the penumbra from each group. Nevertheless, within each group (males, estrus, or diestrus females) the metabolite levels are nearly always significantly different when comparing dissimilar ROIs – such as comparing infarct to penumbra – and these ROIs showed significant differences from metabolite levels in the non-stroke cortex (summarized in Tables S1 and S3 in Supporting Information).

The three clusters (infarct, penumbra, and cortex) were significantly different from one another within each animal group (estrus and diestrus females, and males) for nearly all metabolites. This trend is highlighted by the metabolites in Fig. 1, which includes the lipid distribution (as plotted in Fig. 3A and summarized in Table S3). Additional metabolites, such as lactate, glutamate, ATP+ADP, aggregated protein content, S, Cl, K, and Zn also followed this general trend of deviations from normal levels through the penumbra and continuing into the infarct core, but not all reach statistically significant changes at 24-hours post-stroke (Pushie et al., 2020). Nevertheless, the infarct and penumbra ROIs generally demonstrated the same trends in metabolite concentrations across all 3 animal groups (Table S3). The one exception to this was seen in copper concentrations, however, due to the low detection limits for copper, these findings were consistent with the off-sample regions (background), making the concentrations used for infarct and penumbra comparison unreliable. Quantification of the metabolites in the penumbra revealed a significant difference for glycogen concentration and for phosphorus between groups. All other metabolites were not statistically significant. Fig. 3B shows that glycogen levels found in the penumbra of male animals was significantly lower compared to that of estrus females (p -value = 0.0015, Table S3). Phosphorus was significantly higher in the penumbra of estrus females, compared with diestrus females as displayed in Fig. 3 (p -value = 0.0088, Table S3). No significant difference was seen between male and female groups for phosphorus concentrations in the penumbra.

Discussion

The elements identified with XFI and the FTIR-detected metabolites demonstrate distinct differences in concentration and distribution between the infarct core, the penumbra, and contralateral cortex tissue and generally demonstrated that the PT stroke model generates lesions with similar characteristics in male and female mice. Not all metabolites showed significant differences in distribution between infarct core, penumbra compared with cortex at 24-hours post-stroke, however we have demonstrated in a male-only time course study (1 h – 4 weeks post-stroke) that many of the tracked metabolites do show significant changes over longer post-stroke intervals. Despite females having significantly lower body mass compared to males in this study (11 weeks-old) there was negligible difference in the cross-sectional brain areas in the region of the stroke lesion. Previous studies with magnetic resonance imaging found the volume of male mouse brains was 2.5% larger than females (Spring et al., 2007). Furthermore, there was a negligible difference in the cross-sectional area of affected tissue, including when differentiated into infarct core and penumbra.

No significant differences were observed in post-stroke (or post-sham surgery) function, survival, or the number of individuals removed due to exclusion criteria between male or female groups. Sham surgeries did not yield any significant differences in contralateral cortex levels of metabolites or metabolic markers when compared with the contralateral cortex tissue of the PT animals, with the exception of NADH. Male and female groups demonstrated differences in the rate of NADH-linked mitochondrial respiration (male contralateral cortex contained 29% less NADH compared to female contralateral cortex, p -value < 0.0001). Adult mice show differences in NADH-linked mitochondrial respiration, which is region-specific in the brain and this difference was also

observable post-stroke (Arias-Reyes et al., 2019; Gagnard et al., 2018). Sex hormones play a role in regulating energy production in mitochondria as well as resistance to oxidative stress, with females presenting reduced free radical production and increased resistance to oxidative stress (Arias-Reyes et al., 2019; Gagnard et al., 2015).

The observation that total phosphorus content in the ischemic penumbra of estrus females is close to that of normal tissue also requires further investigation and may indicate low molecular weight phosphorus-containing metabolites (such as those involved in energy metabolism) are better retained in these subjects. We are currently developing chemically selective phosphorus K-edge X-ray fluorescence imaging to characterize changes in phosphorus chemical speciation and metabolism following stroke. Combining Gaussian-based clustering to identify the penumbra surrounding the ischemic core aids in the identification of maximal metabolic differences between these ROIs. Copper levels in the cortex are generally very low and close to the current XFI detection limit. Copper levels decrease further within the infarct and penumbra after stroke, leading to Cu quantification that is highly prone to noise and interference from background Cu signals. The observation that the off-sample background signal for Cu fluctuated significantly during analysis (Table S1Q) indicates this element not a reliable marker in the current experiments. This issue was unique to Cu, however, and none of the other elements demonstrated this issue.

Glycogen was increased nearly 1.4x in the female post-stroke penumbra compared to levels in the penumbra of post-stroke males. At 24-hours post-stroke, the glial response following ischemia peaks resulting in astrocyte activity and glial scar formation (Pushie et al., 2020; Hackett et al., 2016). Sex differences have been reported in astrocyte estrogen receptors in the hippocampus leading to an increase in glycogen metabolism (Ibrahim et al., 2020). Elevated glycogen content after an acute ischemic event is common in humans, primates, and mice (Cai et al., 2020) and while glycogen can be utilized to offset energy needs during subsequent ischemic conditions (Brown, 2004; Brown et al., 2005) its metabolism is impaired after periods of hypoxia or after ischemic stroke (Hossain et al., 2014). Cordeau et al. have also demonstrated estrus-dependent changes by 24-hours post-stroke, particularly in astrocytes, in mice subjected to the MCAO stroke model (Cordeau et al., 2008).

Estrus females also demonstrated a significant increase of 1.3x in total phosphorus content over the levels of this element in the penumbra of diestrus females (differences with the male penumbra showed a similar trend to the diestrus females, but this did not approach statistical significance).

Conclusions

The majority of animal stroke research to-date has been performed on male subjects, however there has been a growing appreciation over the past decade that the pathophysiology of stroke demonstrates sex-linked differences (Bushnell et al., 2018). In human stroke cases women are more likely to suffer a stroke than men and stroke mortality is higher among women, although the global lifetime risk of stroke (over the age of 25) is $24.9\% \pm 1.3\%$ for males and $24.7\% \pm 1.3\%$ for females (GBD, 2016). Women experience poorer functional recovery and reduced quality of life after a stroke compared with men (Reeves et al., 2008; Gall et al., 2018). A benefit of animal models is the ability to control experimental variables, along with less overall variability in experimental subjects compared with individuals in the human population, thus offering reduced complexity when considering sex-linked differences, but without the ability to recapitulate the complex nature of sex or gender expression among human individuals (Rexrode et al., 2022).

The photothrombotic stroke model yielded highly reproducible stroke lesion sizes across all subjects, irrespective of total body mass, sex, or estrus/diestrus status in females. Of the metabolites and biomarkers that were tracked (lipids, protein, aggregated protein, lactate, glycogen,

glutamate, ATP+ADP, NADH, as well as total elemental composition of phosphorus, sulfur, chlorine, potassium, calcium, iron, and zinc) the infarct core of females (regardless of estrous status) and males demonstrated comparable post-stroke changes at 24 h across all groups. Moreover, the surrounding ischemic penumbra, which is a common target for clinical and pre-clinical intervention and treatment, was also similar between males and females, with the exception of glycogen and phosphorus content – suggesting that within these experimental bounds, the body of past experimental findings from male animals may be generally applicable to females. Future studies will determine whether the elevated glycogen in the penumbra of estrus females may confer a neuroprotective advantage or improve their functional outcomes.

CRedit authorship contribution statement

Julia M. Newton: Formal analysis, Investigation, Resources, Writing – original draft, Writing – reviewing and editing. **M. Jake Pushie:** Software, Validation, Formal analysis, Investigation, Data curation, Writing – original draft, Writing – reviewing and editing, Project administration. **Nicole J. Sylvain:** Conceptualization, Methodology, Validation, Formal analysis, Investigation, Resources, Data curation, Writing – reviewing and editing, Project administration. **Huishu Hou:** Methodology, Validation, Investigation, Resources, Writing – reviewing and editing. **Sharleen Weese Maley:** Conceptualization, Writing – reviewing and editing, Project administration. **Michael E Kelly:** Writing – reviewing and editing, Supervision, Funding acquisition.

Acknowledgements

MEK is supported by the Saskatchewan Research Chair in Clinical Stroke Research which is funded by the Heart and Stroke Foundation, Saskatchewan Health Research Foundation, and the University of Saskatchewan College of Medicine. JN was supported through a Biomedical Summer Research Project award at the University of Saskatchewan College of Medicine. Use of the Stanford Synchrotron Radiation Light-source, SLAC National Accelerator Laboratory, is supported by the U.S. Department of Energy, Office of Science, Office of Basic Energy Sciences under Contract No. DE-AC02-76SF00515. The SSRL Structural Molecular Biology Program is supported by the DOE Office of Biological and Environmental Research, and by the National Institutes of Health, National Institute of General Medical Sciences (P30GM133894). The contents of this publication are solely the responsibility of the authors and do not necessarily represent the official views of NIGMS or NIH. Part of this research was performed at the Canadian Light Source, a national research facility of the University of Saskatchewan, which is supported by the Canada Foundation for Innovation (CFI), the Natural Sciences and Engineering Research Council (NSERC), the National Research Council (NRC), the Canadian Institutes of Health Research (CIHR), the Government of Saskatchewan, and the University of Saskatchewan.

Appendix A. Supporting information

Supplementary data associated with this article can be found in the online version at [doi:10.1016/j.ibneur.2022.07.006](https://doi.org/10.1016/j.ibneur.2022.07.006).

References

Arias-Reyes, C., Losantos-Ramos, K., Gonzales, M., Furrer, D., Soliz, J., 2019. NADH-linked mitochondrial respiration in the developing mouse brain is sex-, age- and tissue-dependent. *Respir. Physiol. Neurobiol.* 266, 156–162.
 Beery, A.K., Zucker, I., 2011. Sex bias in neuroscience and biomedical research. *Neurosci. Biobehav. Rev.* 35 (3), 565–572.
 Brown, A.M., 2004. Brain glycogen re-awakened. *J. Neurochem.* 89, 537–552.
 Brown, A.M., Sickmann, H.M., Fosgerau, K., Lund, T.M., Schousboe, A., Waagepetersen, H.S., Ransom, B.R., 2005. Astrocyte glycogen metabolism is required for neural activity during aglycemia or intense stimulation in mouse white matter. *J. Neurosci. Res.* 79, 74–80.

Bushnell, C.D., Chaturvedi, S., Gage, K.R., Herson, P.S., Hurn, P.D., Jiménez, M.C., Kittner, S.J., Madsen, T.E., McCullough, L.D., McDermott, M., Reeves, M.J., 2018. Sex differences in stroke: challenges and opportunities. *J. Cereb. Blood Flow. Metab.* 38, 2179–2191.
 Cai, Y., Guo, H., Fan, Z., Zhang, X., Wu, D., Tang, W., Gu, T., Wang, S., Yin, A., Tao, L., Ji, X., 2020. Glycogenolysis is crucial for astrocytic glycogen accumulation and brain damage after reperfusion in ischemic stroke. *iScience* 23, 101136.
 Caine, S., Hackett, M.J., Hou, H., Kumar, S., Maley, J., Ivanishvili, Z., Suen, B., Szmigielski, A., Jiang, Z., Sylvain, N.J., Nichol, H., Kelly, M.E., 2016. A novel multimodal platform to image molecular and elemental alterations in ischemic stroke. *Neurobiol. Dis.* 91, 132–142.
 Caligioni, C.S., 2009. Assessing reproductive status/stages in mice. *Curr. Protoc. Neurosci.* 48, A–41.
 Conover, W.J., 1999. *Practical Nonparametric Statistics*, 3rd edn..., Wiley, Hoboken, NJ.
 Conover W.J. and Iman R.L. (1979) On multiple-comparisons procedures. Technical report LA-7677-MS, Los Alamos Scientific Laboratory.
 Cordeau Jr, P., Lalancette-Hébert, M., Weng, Y.C., Kriz, J., 2008. Live imaging of neuroinflammation reveals sex and estrogen effects on astrocyte response to ischemic injury. *Stroke* 39, 935–942.
 Crawford, A.M., Sylvain, N.J., Hou, H., Hackett, M.J., Pushie, M.J., Pickering, I.J., George, G.N., Kelly, M.E., 2018. A comparison of parametric and integrative approaches for X-ray fluorescence analysis applied to a Stroke model. *J. Synchrotron Rad.* 25, 1780–1789.
 Demsar, J., et al., 2013. Orange: data mining toolbox in python. *J. Mach. Learn. Res.* 14, 2349–2353.
 Diler, A.S., Uzüm, G., Akgün Dar, K., Aksu, U., Atukeren, P., Ziylan, Y.Z., 2007. Sex differences in modulating blood brain barrier permeability by NO in pentylenetetrazol-induced epileptic seizures. *Life Sci.* 80, 1274–1281.
 Dotson, A.L., Wang, J., Saugstad, J., Murphy, S.J., Offner, H., 2015. Splenectomy reduces infarct volume and neuroinflammation in male but not female mice in experimental stroke. *J. Neuroimmunol.* 278, 289–298.
 Du, L., Bayir, H., Lai, Y., Zhang, X., Kochanek, P.M., Watkins, S.C., Graham, S.H., Clark, R.S., 2004. Innate gender-based proclivity in response to cytotoxicity and programmed cell death pathway. *J. Biol. Chem.* 279, 38563–38570.
 Feigin, V.L., Brainin, M., Norrving, B., Martins, S., Sacco, R.L., Hacke, W., Lindsay, P., 2022. World stroke organization (WSO): global stroke fact sheet 2022. *Int. J. Stroke* 17 (1), 18–29.
 Gagnard, P., Saviouroux, S., Liere, P., Pianos, A., Therond, P., Schumacher, M., Slama, A., Guennoun, R., 2015. Effect of sex differences on brain mitochondrial function and its suppression by Ovariectomy and in aged mice. *Endocrinology* 156, 2893–2904.
 Gagnard, P., Frechou, M., Liere, P., Therond, P., Schumacher, M., Slama, A., Guennoun, R., 2018. Sex differences in brain mitochondrial metabolism: influence of endogenous steroids and stroke. *J. Neuroendocrinol.* 30.
 Gall, S., Phan, H., Madsen, T.E., Reeves, M., Rist, P., Jimenez, M., Lichtman, J., Dong, L., Lisabeth, L.D., 2018. Focused update of sex differences in patient reported outcome measures after stroke. *Stroke* 49, 531–535.
 GBD, 2016. Lifetime Risk of Stroke Collaborators. (2018) Global, regional, and country-specific lifetime risks of stroke, 1990 and 2016. *NEJM* 379, 2429–2437.
 Girijala, R.L., Sohrabji, F., Bush, R.L., 2017. Sex differences in stroke: review of current knowledge and evidence. *Vasc. Med.* 22 (2), 135–145.
 Haast, R.A., Gustafson, D.R., Kiliaan, A.J., 2012. Sex differences in stroke. *J. Cereb. Blood Flow. Metab.* 32, 2100–2107.
 Hackett, M.J., McQuillan, J.A., El-Assaad, F., Aitken, J.B., Levina, A., Cohen, D.D., Siegle, R., Carter, E.A., Grau, G.E., Hunt, N.H., Lay, P.A., 2011. Chemical alterations to murine brain tissue induced by formalin fixation: implications for biospectroscopic imaging and mapping studies of disease pathogenesis. *Analyst* 136, 2941–2952.
 Hackett, M.J., Sylvain, N.J., Hou, H., Caine, S., Alaverdashvili, M., Pushie, M.J., Kelly, M.E., 2016. Concurrent glycogen and lactate imaging with FTIR spectroscopy to spatially localize metabolic parameters of the glial response following brain ischemia. *Anal. Chem.* 88, 10949–10956.
 Hossain, M.I., Roulston, C.L., Stapleton, D.I., 2014. Molecular basis of impaired glycogen metabolism during ischemic stroke and hypoxia. *PLoS One* 9, e97570.
 Ibrahim, M.M., Bheemanapally, K., Sylvester, P.W., Briski, K.P., 2020. Sex-specific estrogen regulation of hypothalamic astrocyte estrogen receptor expression and glycogen metabolism in rats. *Mol. Cell. Endocrinol.* 504, 110703.
 Kruskal, W.H., Wallis, W.A., 1952. Use of ranks in one-criterion variance analysis. *J. Am. Stat. Assoc.* 47, 583–621.
 Lyden, P., Buchan, A., Boltze, J., Fisher, M., 2021. Top priorities for cerebroprotective studies—A paradigm shift: report from STAIR XI. *Stroke* 52 (9), 3063–3071.
 Manwani, B., McCullough, L.D., 2011. Sexual dimorphism in ischemic stroke: lessons from the laboratory. *Women's Health* 7, 319–339.
 Oztas, B., Camurcu, S., Kaya, M., 1992. Influence of sex on the blood brain barrier permeability during bicuculline-induced seizures. *Int. J. Neurosci.* 65, 131–139.
 Pushie, M.J., Messmer, M., Sylvain, N.J., Heppner, J., Newton, J.M., Hou, H., Hackett, M. J., Kelly, M.E., Peeling, L. (2022a) Multimodal imaging of hemorrhagic transformation biomarkers in an ischemic stroke model. *Metallomics*, 14, mfac007.
 Pushie, M.J., Sylvain, N.J., Hou, H., Hackett, M.J., Kelly, M.E., Webb, S.M. (2022b) X-ray fluorescence microscopy methods for biological tissues. *Metallomics*, 14, mfac032.
 Pushie, M.J., Meher, V.R., Sylvain, N.J., Hou, H., Kudryk, A.T., Kelly, M.E., Auer, R.N., 2018a. Histological and elemental changes in ischemic stroke. *Acute Neuronal Injury*. Springer, Cham., pp. 153–171.
 Pushie, M.J., Crawford, A.M., Sylvain, N.J., Hou, H., Hackett, M.J., George, G.N., Kelly, M.E., 2018b. Revealing the penumbra through imaging elemental markers of cellular metabolism in an ischemic stroke model. *ACS Chem. Neurosci.* 9, 886–893.

- Pushie, M.J., Sylvain, N.J., Hou, H., Caine, S., Hackett, M.J., Kelly, M.E., 2020. Tracking elemental changes in an ischemic stroke model with X-ray fluorescence imaging. *Sci. Rep.* 10 (1), 1–14.
- Reeves, M.J., Bushnell, C.D., Howard, G., Gargano, J.W., Duncan, P.W., Lynch, G., Khatiwoda, A., Lisabeth, L., 2008. Sex differences in stroke: epidemiology, clinical presentation, medical care, and outcomes. *Lancet Neurol.* 7, 915–926.
- Rexrode, K.M., Madsen, T.E., Yu, A.Y., Carcel, C., Lichtman, J.H., Miller, E.C., 2022. The impact of sex and gender on stroke. *Circ. Res.* 130, 512–528.
- Spring, S., Lerch, J.P., Henkelman, R.M., 2007. Sexual dimorphism revealed in the structure of the mouse brain using three-dimensional magnetic resonance imaging. *Neuroimage* 35, 1424–1433.
- Wald, C., & Wu, C. (2010). *Of mice and women: the bias in animal models.*
- Webb, S.M., 2011. The MicroAnalysis Toolkit: X-ray fluorescence image processing software. *Am. Inst. Phys. Conf. Proc.* 1365196–1365199.
- Winship, I.R., Murphy, T.H., 2008. In vivo calcium imaging reveals functional rewiring of single somatosensory neurons after stroke. *J. Neurosci.* 28, 6592–6606.
- Yang, S.H., Liu, R., 2021. Four decades of ischemic penumbra and its implication for ischemic stroke. *Transl. Stroke Res.* 12 (6), 937–945.